Nonlinear Optical Spin Hall Effect and Long-Range Spin Transport in Polariton Lasers

E. Kammann,[1] T. C. H. Liew,[2] H. Ohadi,[1] P. Cilibrizzi,[1] P. Tsotsis,[3] Z. Hatzopoulos,[3,4] P. G. Savvidis,[1,3,5] A. V. Kavokin,[1,6] and P. G. Lagoudakis[1,*]

[1]*School of Physics and Astronomy, University of Southampton, Southampton, SO17 1BJ, United Kingdom*
[2]*School of Physical and Mathematical Sciences, Nanyang Technological University, 637371, Singapore*
[3]*Microelectronics Research Group, IESL-FORTH, P.O. Box 1527, 71110 Heraklion, Crete, Greece*
[4]*Department of Physics, University of Crete, 71003 Heraklion, Crete, Greece*
[5]*Department of Materials Science and Technology, University of Crete, P.O. Box 2208, 71003 Heraklion, Greece*
[6]*Spin Optics Laboratory, St. Petersburg State University, 1, Ulianovskaya, St. Peterbsurg, 198504, Russia*
(Received 21 April 2012; published 18 July 2012)

We report on the experimental observation of the nonlinear analogue of the optical spin Hall effect under highly nonresonant circularly polarized excitation of an exciton-polariton condensate in a GaAs/AlGaAs microcavity. The circularly polarized polariton condensates propagate over macroscopic distances, while the collective condensate spins coherently precess around an effective magnetic field in the sample plane performing up to four complete revolutions.

DOI: 10.1103/PhysRevLett.109.036404 PACS numbers: 71.36.+c, 72.25.Dc, 72.25.Fe

Semiconductor microcavities in the strong coupling regime are excellent candidates for designing novel ''spinoptronic'' devices due to their strong optical nonlinearity, unusual polarization properties, and fast spin dynamics. The first steps toward the fabrication of spin-based switching have been recently demonstrated [1–3]. An important goal for the development of integrated devices is coherent spin transport. Being neutrally charged, exciton-polaritons have a significantly smaller scattering cross section with atomic cores than electrons in a metal. Strongly suppressed scattering, which was interpreted as superfluidity, has been recently demonstrated in polaritons [4]. Fabrication of high finesse microcavities has allowed ballistic polariton propagation and long-range order extending over macroscopic distances far beyond the excitation area [5]. Here, we show the coherent transport of the spin vector in propagating polariton condensates. We observe ballistic propagation of spin polarized polaritons over distances of a few hundred microns. The observed nondissipative long-range spin transport is caused by mass transport of exciton-polaritons, which distinguishes the phenomenon we observe from spin superfluidity reported for ^{3}He [6], where the spin transport is decoupled from the mass transport.

The polarization state of exciton-polaritons can be described within the pseudospin formalism [7]. Polaritons possess a spin with two possible projections on the structural growth axis of the microcavity. The polarization of the emitted light gives direct access to the pseudospin state, which is fully characterized by the four-component Stokes vector $\vec{s} = (s_0, s_x, s_y, s_z)$. Here, s_0 is the total degree of polarization, and $s_{x,y,z} = (I_{H,D,\circlearrowleft} - I_{V,A,\circlearrowleft})/I_{\mathrm{tot}}$. $I_{H,D,\circlearrowleft}$ and $I_{V,A,\circlearrowleft}$ are the measured intensities in the horizontal and vertical, diagonal and antidiagonal, and the two circular polarization components, and I_{tot} is the total emission intensity.

The energies of the linear polarizations are split due to the long-range exciton interaction [8] and the transverse electric and magnetic mode splitting of the cavity [9]. This splitting (Δ_{LT}) vanishes for the normal incidence and acts as a directionally dependent effective magnetic field in the plane of the microcavity ($\vec{H}_{\mathrm{eff}} = \frac{\hbar}{\mu_{BG}}\vec{\Omega}_k$), which causes the precession of the pseudospin for polaritons with a finite k vector. $\vec{\Omega}_k$ has the components:

$$\Omega_x = \frac{\Delta_{\mathrm{LT}}}{\hbar k^2}(k_x^2 - k_y^2), \qquad \Omega_y = \frac{\Delta_{\mathrm{LT}}}{\hbar k^2} k_x k_y, \tag{1}$$

where $\vec{k} = (k_x, k_y)$ is the in-plane wave vector of the polariton. The effective magnetic field can be utilized to generate polarization patterns [10,11] as well as spin-polarized vortices [11] and solitons [12]. In a radially expanding polariton condensate, a spin structure is generated that can be described by the equation

$$v_r \frac{\partial \vec{\sigma}(\vec{r})}{\partial r} = \vec{\sigma}(\vec{r}) \times \vec{\Omega}_k, \tag{2}$$

where v_r is the radial velocity, $\vec{\sigma}$ is the pseudospin vector. $\vec{H}_{\mathrm{eff}}$ shown in Figs. 1(a) and 1(b) illustrates the precession of a circularly polarized polariton with a finite k vector. An analogy to the intrinsic spin Hall effect in doped quantum wells, where the spin of moving electrons or holes interacts with the Dresselhaus and Rashba fields [13,14], is apparent. The phenomenon described here is called the optical spin Hall effect and was first predicted by Kavokin and coworkers [15]. Hereafter, the experimental observations followed in a semiconductor microcavity in the strong coupling regime [16] and a purely photonic cavity [17] under the resonant injection of polaritons and photons. This series relies on resonant Rayleigh scattering to mediate anisotropic distribution of spin in real and momentum

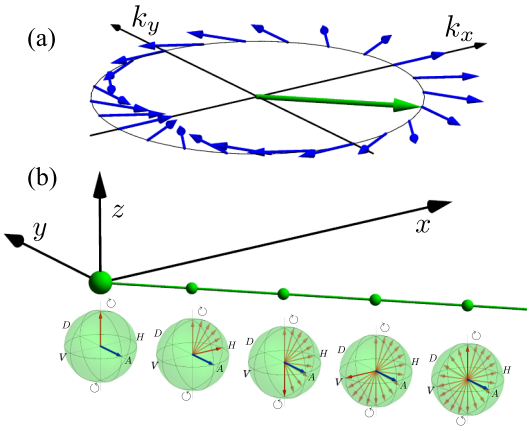

FIG. 1 (color online). (a) The blue [dark gray] arrows show the distribution of the effective magnetic field caused by the TE-TM splitting in momentum space. (b) A polariton is injected with circular polarization (marked by red [medium gray] arrows) at the center of the excitation spot and moving outward [with the k vector shown in green [light gray] in (a)] experiences a spin precession around the effective magnetic field. The pseudospin vector in the Poincaré sphere at points where $\frac{\Delta_{LT} m}{\hbar^2 k}|\vec{r}| = 0$, $\pi/2$, π, $3\pi/2$, 2π is shown. Here m is the effective polariton mass.

space and, therefore, it is an analogy for the extrinsic spin Hall effect first predicted by Dyakonov and Perel in 1971 [18]. In this Letter, we show a method to observe the optical spin Hall effect without the necessity of Rayleigh scattering and, therefore, a kind of intrinsic optical spin Hall effect. We create a propagating circularly polarized polariton condensate by means of nonresonant optical excitation. As polaritons ballistically propagate through the sample, their spin precesses coherently about the effective magnetic field lying in the plane of the sample, giving rise to a distinct spin pattern in real space. It is worth mentioning the one fundamental difference between the optical spin Hall effect and the spin Hall effect: While the spin Hall effect causes the separation of unpolarized carriers in spin up and spin down fractions, the optical spin Hall effect rotates the direction of the polariton pseudospin (Stokes vector) in the Poincaré sphere.

We use a $5\lambda/4$ AlGaAs/GaAs microcavity with a Rabi splitting of $\sim$9 meV and a cavity photon lifetime of $\sim$9 ps [19]. A circularly polarized continuous wave excitation was tuned to a reflection minimum of the Bragg mirror outside the high reflectivity region and focused to a $\sim$5-μm diameter spot through a 0.2 NA objective. All experiments were performed at $\sim$7 K using a cold finger cryostat. The excitation laser was intensity modulated using an acousto-optic modulator at 10 kHz with a 5% duty cycle to reduce sample heating. The emission was spectrally separated from the excitation laser and imaged onto a water-cooled CCD or sent to a 300 mm imaging spectrometer. Calibrated wave plates and a polarizer were positioned in the detection path to analyze the polarization.

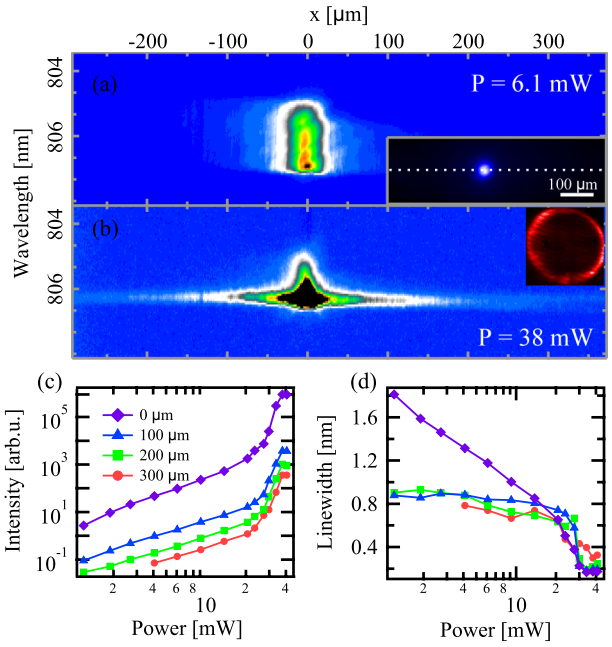

FIG. 2 (color online). Energy-resolved emission of a cross section through the image of the spot [inset in (a)] below (a) and above threshold (b). The inset in (b) shows the far-field emission above threshold. (c) Emission intensity at various distances from the excitation spot show a superlinear increase at a threshold of about 25 mW. (d) The linewidth as a function of power rapidly drops at the threshold [color legend in (c)].

When the sample is excited with a sufficiently small excitation spot ($\lesssim 10$ μm), the repulsive interaction causes a strong blueshift of the condensate and radial ballistic propagation of condensed polaritons out of the excitation spot [20]. Figure 2 shows the energy-resolved emission of a cross section through the excitation spot for below (a) and above (b) threshold power. Above the threshold power, the far-field emission forms a ring in reciprocal space [inset in Fig. 2(b)]. Spatially resolved dispersions reveal that polaritons condense at $k = 0$ at a strongly blueshifted energy, due to repulsive interactions with the exciton reservoir. Outside the pump spot the potential energy is converted to kinetic energy, and the blueshift of the condensate determines the in-plane wave vector. Spatially filtered energy-momentum dispersions are supplied in Ref. [21]. The collected emission spectra at different distances from the excitation area show a superlinear increase (c) and a rapidly dropping linewidth (d) at the photoluminescence threshold as far as 300 μm away from the excitation spot. These features are characteristic for lasing, condensation, and buildup of coherence.

In Ref. [22] we showed that the spin of the excitation laser is conserved to a certain degree under nonresonant circularly polarized excitation, while the phase correlation between the spin up and spin down polaritons is lost. We utilize this phenomenon to nonresonantly form polariton condensates with a collective spin state and study their

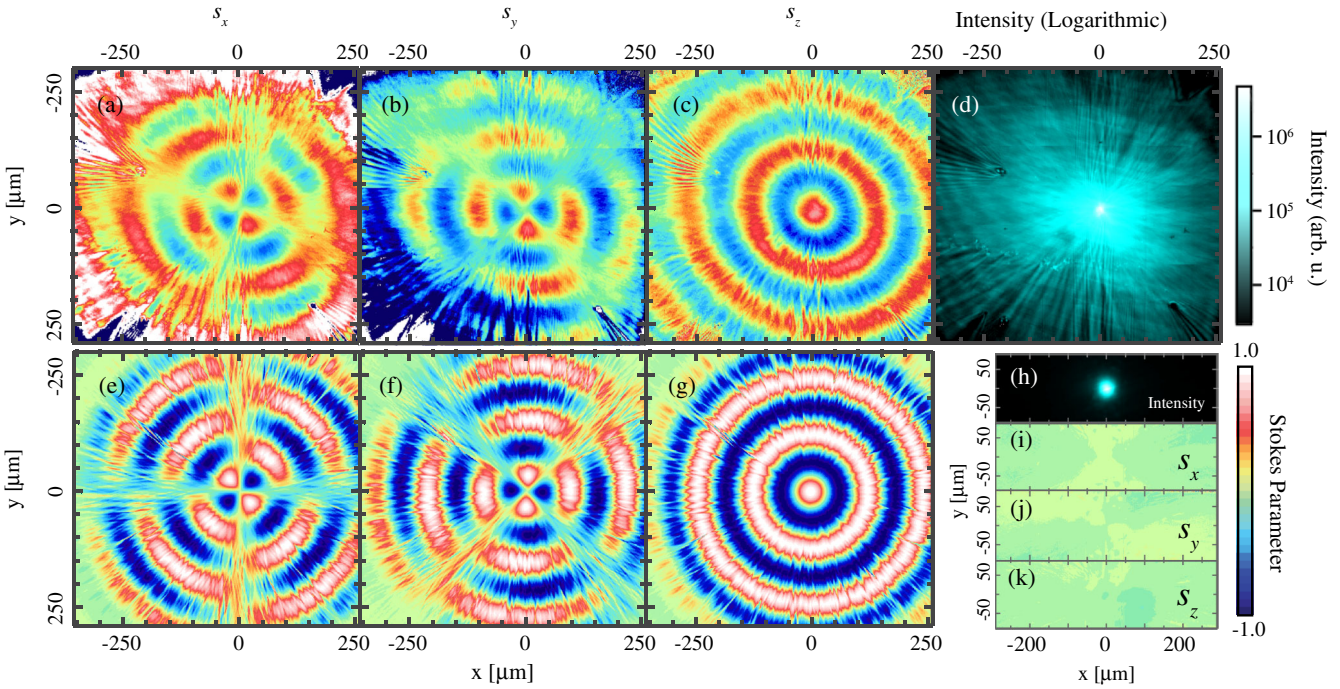

FIG. 3 (color online). (a) Experimental data (a)–(c) and numerical simulations (e)–(g) of the Stokes parameters of the emission of a polariton condensate non-resonantly excited with circularly polarized laser at $2 \times P_{\mathrm{thr}}$, s_x (a),(e) s_y (b),(f) s_z (c),(g). (d) Emission intensity on a logarithmic color scale. Below the P_{thr} the effect cannot be observed, due to the broad k-space distribution (h)–(k).

long-range spin transport. The transverse electric and the transverse magnetic photon mode splitting causes the rotation of the spin as the polaritons propagate through the sample, due to the optical spin Hall effect [15]. Figure 3(a) shows the integrated emission mapped in the near field. The linear components of the Stokes vector (s_x and s_y) exhibit a cartwheel pattern [Figs. 3(b) and 3(c)]. The circular component [Fig. 3(d)] reveals up to four revolutions of the pseudospin around the effective magnetic field within the polariton lifetime and a circular symmetric ring pattern. The spacing of two successive rings of the same circular polarization ($\delta r_{\circlearrowleft,\circlearrowleft}$) is determined by the solution to Eq. (2) and, therefore, depends on the radial velocity of the polaritons and the TE-TM splitting that corresponds to the in-plane k vector ($\delta r_{\circlearrowleft,\circlearrowleft} = \frac{\pi\hbar^2}{m}\frac{k}{\Delta_{\mathrm{LT}}}$).

To demonstrate the nonlinearity of the effect, the same measurement was performed below the threshold. Here, polaritons are evenly distributed in k space and, therefore, experience different effective magnetic fields. Figure 3(h) depicts the intensity below threshold. The Stokes components s_x, s_y, and s_z are displayed in Figs. 3(i)–3(k), respectively. In case of a linearly polarized excitation laser above threshold, the ring condensate was randomly polarized within the excitation area [22,23] and no spin pattern was observed.

Theoretically, the spatial dynamics of polariton condensates is described by a Gross-Pitaevskii type equation for the polariton field [24], which should be coupled to a reservoir of hot excitons that are excited by the nonresonant pump [25]. The Gross-Pitaevskii equation is generalized to include the polarization degree of freedom [26] of polariton condensates:

$$
\begin{aligned}
i\hbar\frac{d\Psi_\sigma(x,y,t)}{dt} = \Big(&-\frac{\hbar^2}{2m}\nabla^2 - i\hbar\frac{\gamma}{2} + \alpha|\Psi_\sigma(x,y,t)|^2 \\
&+ \Big(g_R + i\hbar\frac{r}{2}\Big)n_\sigma(x,y,t) \\
&+ \hbar G P_\sigma(x,y,t) + V(x,y)\Big)\Psi_\sigma(x,y,t) \\
&+ \frac{\Delta_{\mathrm{LT}}}{k_{\mathrm{LT}}^2}\Big(i\frac{\partial}{\partial x} + \sigma\frac{\partial}{\partial y}\Big)^2\Psi_{-\sigma}(x,y,t). \qquad (3)
\end{aligned}
$$

$\Psi_\sigma(x,y,t)$ represents the mean field of polaritons, with $\sigma = \pm$ representing the spin of polaritons. We approximate the polariton dispersion as parabolic, with effective mass m, which is valid since the observed energies and in-plane wave vectors in the experiment lie in the parabolic part of the dispersion. γ represents the polariton decay rate. α is the polariton-polariton interaction strength, which was assumed spin-independent for simplicity (the interactions between polaritons with opposite spins are much weaker [27]. $n_\sigma(x,y,t)$ is the density of the hot exciton reservoir, which may be polarized depending on the pump polarization but is assumed incoherent. g_R represents the effect of repulsive interactions between the reservoir and polaritons (also assumed negligible for oppositely polarized spins) and r is the condensation rate, representing the process where hot excitons condense into polaritons. An additional

pump-induced shift is described by the interaction constant G, where $P_\sigma(x, y, t)$ is the spatial pump distribution [25]. $V(x, y)$ represents the static disorder potential typical in semiconductor microcavities, which is chosen as a random Gaussian-correlated potential [16]. The last term represents the presence of longitudinal-transverse splitting of the polariton modes [9,15], which is assumed to increase with the square of the in-plane wave vector (parabolic approximation).

The evolution of the hot exciton density is given by the rate equation:

$$\frac{dn_\sigma(x, y, t)}{dt} = [-\Gamma + r|\Psi_\sigma(x, y, t)|^2]n_\sigma(x, y, t) + P_\sigma(x, y, t), \quad (4)$$

where Γ is the reservoir decay rate. We consider a circularly polarized continuous wave pump. Starting from a random initial condition, the time evolution of the system can be calculated numerically until a steady state is reached, which is independent of the initial condition. Figures 3(e) and 3(f) show the distribution of the calculated Stokes vectors in space [28].

Although we have included a disorder potential in our theoretical model, the Rayleigh scattering of polaritons with disorder is not necessary for the observation of the multiple rings and cartwheel structure of the polarization in space. This is in contrast to the original demonstration of the optical spin Hall effect [15–17], where Rayleigh scattering was required to populate a ring in reciprocal space. In our case, polaritons condense at the laser spot position with a blueshifted energy due to their interactions with uncondensed hot excitons. While these hot excitons experience a limited diffusion, polaritons ballistically fly away from the laser spot, converting this interaction energy into kinetic energy. The kinetic energy is characterized by the nonzero wave vector of polaritons, which due to the circular symmetry of the excitation corresponds to a ring in reciprocal space.

The disorder potential does, however, have a noticeable effect on the fine structure of the polarization in space. Without disorder, similar calculations reveal smooth rings with perfect circular symmetry in the s_z distribution (and smooth profiles with order 2 rotational symmetry in the s_x and s_y distributions). The addition of disorder gives the rings a noticeable texture and breaks the perfect circular symmetry (leaving only approximately symmetrical distributions). The observed texture is similar to that recorded experimentally. Although this indicates that a small amount of scattering with disorder is present, it is clear that we are in a regime of weak scattering or it would not be possible to observe such clear polarization patterns over such distances.

In conclusion, we have experimentally demonstrated the nonlinear optical spin Hall effect in a polariton condensate, with remarkable agreement with the theoretical prediction. The nonresonant circular excitation allows the excitation of a ring in reciprocal space without the need for large amounts of disorder. Polariton spins propagate ballistically over a 300-μm distance with minimal scattering and minimal loss of spin information. This record confirms the great potential of semiconductor microcavities for the fabrication of spinoptronic devices.

The authors acknowledge the Marie Curie ITNs Spinoptronics and Clermont IV as well as the EPSRC through Contract No. EP/F026455/1 for funding. A. V. K. thanks the Royal Society Leverhulme fellowship. P. G. S. acknowledges funding from the EU Social Fund and Greek National Resources (EPEAEK II, HRAKLEITOS II). E. K. acknowledges discussions with Peter Eldridge.

*pavlos.lagoudakis@soton.ac.uk

[1] P. G. Lagoudakis, P. G. Savvidis, J. J. Baumberg, D. M. Whittaker, P. R. Eastham, M. S. Skolnick, and J. S. Roberts, Phys. Rev. B **65**, 161310 (2002).
[2] A. Amo, T. C. H. Liew, C. Adrados, R. Houdré, E. Giacobino, A. V. Kavokin, and A. Bramati, Nature Photon. **4**, 361 (2010).
[3] C. Adrados, T. C. H. Liew, A. Amo, M. D. Martín, D. Sanvitto, C. Antón, E. Giacobino, A. Kavokin, A. Bramati, and L. Viña, Phys. Rev. Lett. **107**, 146402 (2011).
[4] A. Amo, J. Lefrere, S. Pigeon, C. Adrados, C. Ciuti, I. Carusotto, R. Houdré, E. Giacobino, and A. Bramati, Nature Phys. **5**, 805 (2009).
[5] E. Wertz, L. Ferrier, D. D. Solnyshkov, R. Johne, D. Sanvitto, A. Lemaître, I. Sagnes, R. Grousson, A. V. Kavokin, P. Senellart, G. Malpuech, and J. Bloch, Nature Phys. **6**, 860 (2010).
[6] A. S. Borovik-Romanov, Y. M. Bun'kov, V. V. Dmitriev, and Y. M. Mukharskii, JETP Lett. **40**, 1033 (1984).
[7] K. V. Kavokin, I. A. Shelykh, A. V. Kavokin, G. Malpuech, and P. Bigenwald, Phys. Rev. Lett. **92**, 017401 (2004).
[8] M. Z. Maialle, E. A. de Andrada e Silva, and L. J. Sham, Phys. Rev. B **47**, 15776 (1993).
[9] G. Panzarini, L. C. Andreani, A. Armitage, D. Baxter, M. S. Skolnick, V. N. Astratov, J. S. Roberts, A. V. Kavokin, M. R. Vladimirova, and M. A. Kaliteevski, Phys. Rev. B **59**, 5082 (1999).
[10] W. Langbein, I. Shelykh, D. Solnyshkov, G. Malpuech, Y. Rubo, and A. Kavokin, Phys. Rev. B **75**, 075323 (2007).
[11] F. Manni, K. G. Lagoudakis, T. K. Paraïso, R. Cerna, Y. Léger, T. C. H. Liew, I. A. Shelykh, A. V. Kavokin, F. Morier- Genoud, and B. Deveaud-Plédran, Phys. Rev. B **83**, 241307 (2011).
[12] R. Hivet, H. Flayac, D. D. Solnyshkov, D. Tanese, T. Boulier, D. Andreoli, E. Giacobino, J. Bloch, A. Bramati, G. Malpuech, and A. Amo, arXiv:1204.3564.
[13] S. Murakami, N. Nagaosa, and S. Zhang, Science **301**, 1348 (2003).
[14] J. Sinova, D. Culcer, Q. Niu, N. A. Sinitsyn, T. Jungwirth, and A. H. MacDonald, Phys. Rev. Lett. **92**, 126603 (2004).
[15] A. Kavokin, G. Malpuech, and M. Glazov, Phys. Rev. Lett. **95**, 136601 (2005).

[16] C. Leyder, M. Romanelli, J. P. Karr, E. Giacobino, T. C. H. Liew, M. M. Glazov, A. V. Kavokin, G. Malpuech, and A. Bramati, Nature Phys. **3**, 628 (2007).
[17] M. Maragkou, C. E. Richards, T. Ostatnický, A. J. D. Grundy, J. Zajac, M. Hugues, W. Langbein, and P. G. Lagoudakis, Opt. Lett. **36**, 1095 (2011).
[18] M. Dyakonov and V. Perel, Phys. Lett. **35A**, 459 (1971).
[19] G. Tosi, G. Christmann, N. G. Berloff, P. Tsotsis, T. Gao, Z. Hatzopoulos, P. G. Savvidis, and J. J. Baumberg, Nature Phys. **8**, 190 (2012).
[20] M. Wouters, I. Carusotto, and C. Ciuti, Phys. Rev. B **77**, 115340 (2008).
[21] See Supplemental Material at http://link.aps.org/supplemental/10.1103/PhysRevLett.109.036404 for spatially filtered dispersions at the excitation spot and 90 μm away.
[22] H. Ohadi, E. Kammann, T. C. H. Liew, K. G. Lagoudakis, A. V. Kavokin, and P. G. Lagoudakis, Phys. Rev. Lett. **109**, 016404 (2012).
[23] J. J. Baumberg, A. V. Kavokin, S. Christopoulos, A. J. D. Grundy, R. Butté, G. Christmann, D. D. Solnyshkov, G. Malpuech, G. Baldassarri Höger von Högersthal, E. Feltin, J. Carlin, and N. Grandjean, Phys. Rev. Lett. **101**, 136409 (2008).
[24] I. Carusotto and C. Ciuti, Phys. Rev. Lett. **93**, 166401 (2004).
[25] M. Wouters and I. Carusotto, Phys. Rev. Lett. **99**, 140402 (2007).
[26] I. A. Shelykh, Y. G. Rubo, G. Malpuech, D. D. Solnyshkov, and A. Kavokin, Phys. Rev. Lett. **97**, 066402 (2006).
[27] C. Ciuti, V. Savona, C. Piermarocchi, A. Quattropani, and P. Schwendimann, Phys. Rev. B **58**, 7926 (1998).
[28] Parameters: $m = 7 \times 10^{-5}$ of the free electron mass, $\Delta_{\mathrm{LT}} = 0.05\,\mathrm{meV}$, $k_{\mathrm{LT}} = 2.05\,\mu\mathrm{m}^{-1}$, $\alpha = 2.4\,\mu\mathrm{eV}\,\mu\mathrm{m}^2$, $\gamma = 0.2\,\mathrm{ps}^1$, $\Gamma = 10\gamma$, $\hbar r = 0.1\,\mathrm{meV}\,\mu\mathrm{m}^{-2}$, $G = 0.03\,\mu\mathrm{m}^2$. The disorder potential was generated with 0.05 meV root mean squared amplitude and 1.5-μm correlation length. The pump intensity was chosen to match the experimentally measured blueshift of the polariton condensate.